

## Supplementary Information for

# **Insights into light and mass transport in nanoparticle- based aerogels: the advantages of monolithic 3D photocatalysts**

*Ana Laura Luna<sup>\*1</sup>, Sotirios Papadopoulos<sup>2</sup>, Till Kyburz<sup>1</sup>, Elena Tervoort<sup>1</sup>, Lukas Novotny<sup>2</sup> and  
Markus Niederberger<sup>1</sup>*

<sup>1</sup>Laboratory for Multifunctional Materials, Department of Materials, ETH Zürich, Vladimir-  
Prelog-Weg 5, 8093 Zürich, Switzerland

<sup>2</sup>Photonics Laboratory, ETH Zürich, CH-8093 Zürich, Switzerland

\* Corresponding author

E-mail address: [ana.laura.luna.barron@alumni.ethz.ch](mailto:ana.laura.luna.barron@alumni.ethz.ch)

## Calculating apparent Quantum efficiency

The apparent quantum efficiency for hydrogen generation was calculated according to the following equation:

$$AQE[\%] = \frac{2 \cdot n_{H_2}}{n_{incident\ photons}} \cdot 100$$

where  $n$  denotes the number of the respective species (hydrogen molecules or incident photons) per second.

The number of hydrogen molecules was calculated by multiplying the  $H_2$  evolution rate expressed  $\text{mol} \cdot \text{s}^{-1}$  times the Avogadro number as follow:

$$n_{H_2} \left[ \frac{\text{molecules of } H_2}{s} \right] = r_{H_2} \cdot N_A$$

The incident number of photons (photon flux) was calculated by measuring the power of the LED at the position of the sample using a thermal power sensor (5 W, Thorlabs) connected to an optical power meter console (PM400, Thorlabs). The active detected area of the sensor was  $1 \text{ cm}^2$ . On the other hand, the projected area of the LED is  $\sim 1 \text{ cm}^2$  (see, inset image in **Figure 4a** of the main text) due to the distance between this and the aerogel. Because of this, we considered light intensity equal to measured LED power.

The LED power ( $p$ ) was measured in  $[mW]$  and converted to  $\left[ \frac{J}{s} \right]$  as follow:

$$p \left[ \frac{J}{s} \right] = I[mW] \cdot 10^{-3}$$

We used a LED wavelength ( $\lambda$ ) of 375 nm. The energy of each photon was obtained with the following equation:

$$E \left[ \frac{J}{\text{photon}} \right] = \frac{h \cdot c}{\lambda}$$

where  $h \left[ \frac{J}{s} \right]$  and  $c \left[ \frac{m}{s} \right]$  is the Planck's constant and the speed of light, respectively. Importantly,  $\lambda$  is expressed in meters $[m]$ .

Thus, the photon flux was calculated dividing the LED power by the energy of each photon as follow:

$$n_{incident\ photons} \left[ \frac{\text{photons}}{s} \right] = \frac{p}{E}$$

To study the H<sub>2</sub> evolution rate and AQE as a function of light intensity, the following intensities were used:

**Table S1.** Incident light power used and their corresponding calculated photon flux. We considered LED power equal to light intensity because the detected area of the sensor is equal to the projected area of the LED as is explained above.

Using top LED		Using top & bottom LEDs	
Power [mW]	Calculated photon flux $\left[\frac{photons}{s}\right]$	Power [mW]	Calculated photon flux $\left[\frac{photons}{s}\right]$
1.61	$3.038 \times 10^{15}$	2.58	$4.87 \times 10^{15}$
4.29	$8.09 \times 10^{15}$	7.62	$1.44 \times 10^{16}$
7.47	$1.41 \times 10^{16}$	13.37	$2.52 \times 10^{16}$
23.66	$4.46 \times 10^{16}$	43.30	$8.17 \times 10^{17}$
51.79	$9.77 \times 10^{16}$	97.36	$1.84 \times 10^{17}$
64.19	$1.21 \times 10^{17}$	122.94	$2.3 \times 10^{17}$

### Calculating the number of anatase nanoparticles in the prepared aerogels and the rate of photons absorbed per nanoparticle.

Each aerogel contains  $67.5 \pm 4$  mg of anatase. Considering a specific density of anatase of  $3.9 \text{ g} \cdot \text{cm}^{-3}$ , the occupied volume by such mass was calculated as follow:

$$V_{occupied} = \frac{0.0675g}{3.9g \cdot cm^{-3}} = 0.0173 \text{ cm}^3$$

The diameter of the anatase nanoparticles was 3 nm, meaning that the volume occupied per nanoparticle is:

$$V_{anatase \text{ nanoparticle}} = \frac{4}{3}\pi(1.5 \times 10^{-7}cm)^3 = 1.41 \times 10^{-20}cm^3$$

The number of anatase nanoparticles

was calculated according to the following equation:

$$n_{nanoparticles} = \frac{V_{occupied}}{V_{anatase \text{ nanoparticle}}} = \frac{0.0173cm^3}{1.42 \times 10^{-20}cm^3} = 1.22 \times 10^{18}$$

Considering the highest photon flux ( $2.3 \times 10^{17} \frac{photons}{s}$ ) used in our experiments, the theoretical rate of photons absorbed per nanoparticle was calculated as follow:

$$\frac{2.3 \times 10^{17} \frac{\text{photons}}{s}}{1.22 \times 10^{18} \frac{\text{particle}}{s}} = 0.19 \frac{\text{photons}}{\text{particle} \cdot s}$$

**Three main reasons why spatial characteristic of scattered light (speckle pattern) was measured in reflection using an optical laser-based setup.**

We choose to measure the aerogel in reflection and not in transmission for three reasons. First, in transmission the ballistic light has very high intensity and obscures the scattering effect. Since we are interested in measuring the diffusing light, looking at the backscattered light omits contribution of the ballistic part that propagates solely in forward direction. Second, if we would image the top side of the disk the ballistic part would be broad (see **Figure 5b** in the main text) due to the focusing at the bottom side. This would cause the diffused and ballistic light to overlap making their distinction more difficult. Third, since diffusing light has random direction of propagation, we expect to observe the same effect in forward- and back-scattering.

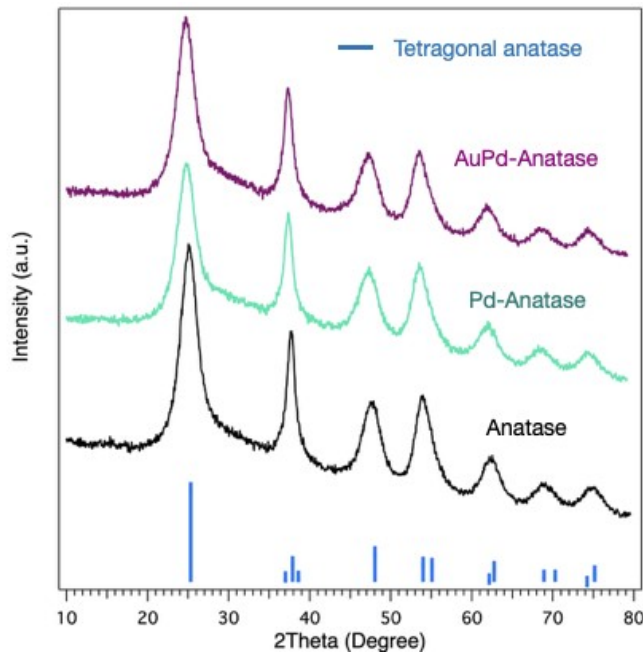


**Figure S1.** X-ray diffractograms of the Pd-anatase, PdAu-anatase, and anatase aerogels. Because of the low metal loading, the reflections corresponding to the metal nanoparticles could not be observed.

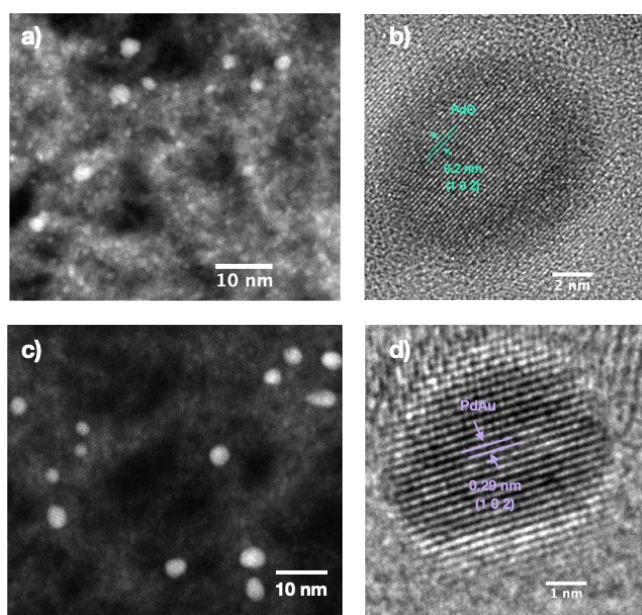


**Figure S2.** HAADF images of (a) Pd-anatase and (c) PdAu-anatase aerogels. HRTEM images of (b) Pd-anatase and (d) PdAu-anatase aerogels.

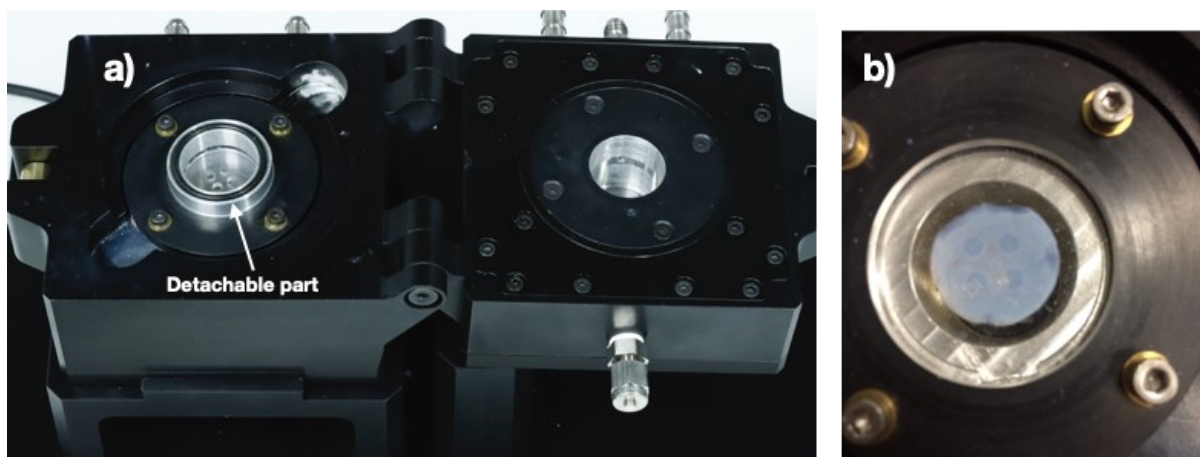


**Figure S3.** (a) Photograph of the open reactor in which the perforated sample holder is observed. (b) Photograph of the sample holder with an anatase aerogel showing that the aerogel monolith covers the four small holes of the holder.

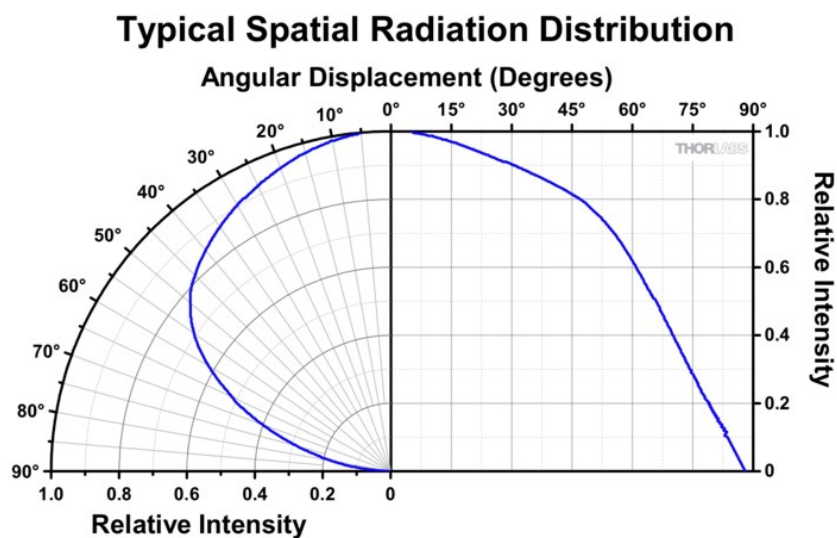


**Figure S4.** Typical spatial radiation distribution of the 375nm LEDs (M375L4) as it was provided by Thorlabs.

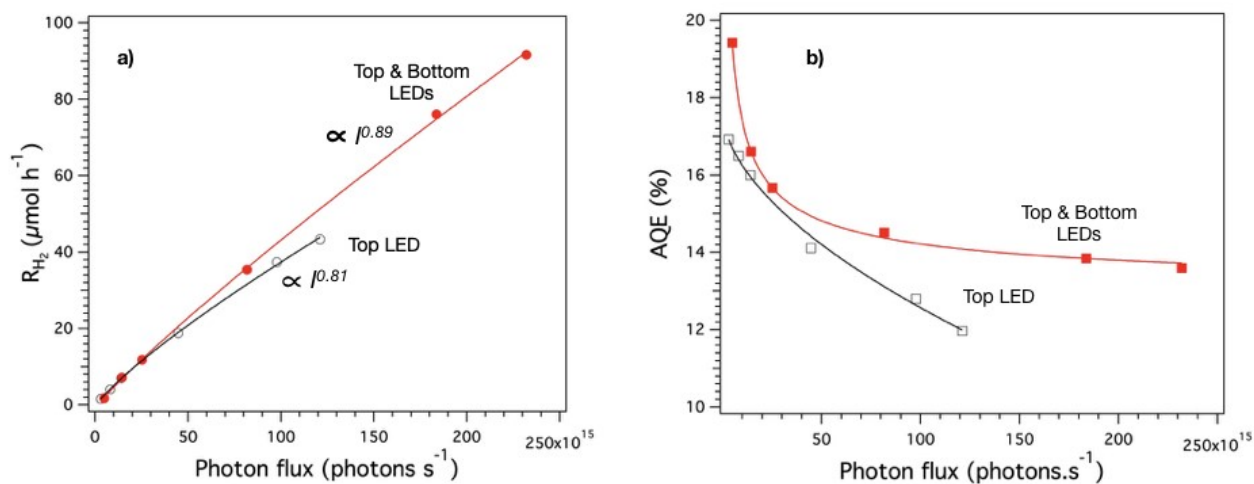


**Figure S5.** Photo-production of H<sub>2</sub> from methanol in a continuous gas-phase reaction over Pd-anatase aerogels as a function of light intensity. (a) H<sub>2</sub> evolution rates and (b) AQE profiles obtained by illuminating the aerogel from the top and from top & bottom.

## Optical setup used for time-resolved measurements.

We measure the temporal characteristics of the diffused light with the scheme presented in **Figure S6a**. A pulsed laser beam is split through a beam splitter into two beams. The reflected beam was measured by the trigger Avalanche Photodetector (trigger APD). The forward collimated beam is driven onto the aerogel. The light was collected with a high NA objective (0.8 NA) misplaced from the excitation beam path to avoid measuring the ballistic component and measure at a point where the diffused light has interacted with the aerogel in a longer path (distance,  $d = 1.03$  cm in FigureXa). The collected light was driven to a second APD and the outputs of both APDs are correlated with a Time-Correlated Single Photon Counting (TCSPC) system PicoHarp 300.

The pulsed light is provided by Coherent Mira-OPO with pulse duration of 200 fs at a repetition rate of 76 MHz. It is important to mention that the measurement resolution in our setup was determined by the time response of the APD (MPD PDM 50), which was measured to be around 180 ps. The Instrument Response Function (IRF) was obtained by correlating the two beams unperturbed (without the aerogel sample). Because the objective was misplaced and the laser beam cannot be collected, to measure the IRF we used a thin glass coverslip edge in the middle of the collimated beam to scatter the light at the same height as the bottom surface of the aerogel disk. Part of the scattered light was then collected by the misplaced objective and measured by the APD. This provides also our reference in time domain (time reference measurement in **Figure S6a**). The IRF obtained in that way is shown in **Figure S6b** as well as the diffusion time-trace acquired. The diffusion should cause a time delay and broadening of the pulse.

Although a small broadening of 10 ps was observed (inset in **Figure S6b**) we cannot confidently claim that this effect is caused by the diffusion in the aerogel. Our limited temporal resolution of our setup didn't allow us to resolve time signatures of diffusion caused by our aerogels precisely and consequently quantify with confidence their diffusive characteristics.

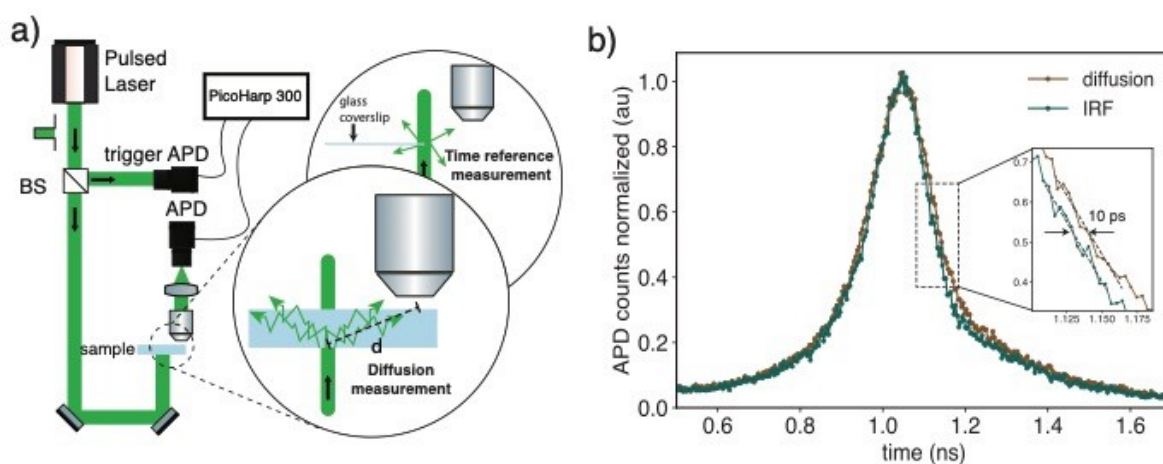


**Figure S6.** (a) Simplified scheme of the optical setup used to measure the temporal characteristics of diffusion. (b) The instrument response function as measured at the optical setup and the resulting measurement of the diffused light. The temporal resolution of the system didn't allow us to confidently quantify the diffusive characteristics.